

Improving medial surfaces for reverse engineering

Vaibhav Kumar^a , Takashi Michikawa^b  and Hiromasa Suzuki^c 

^aAMADA Co., LTD; ^bOsaka University; ^cThe University of Tokyo

ABSTRACT

Common medial axis transform methods create two artifacts: shrinkage of the end of surfaces and small dent at junctions. They are due to the definition of medial axis transforms and they are bottlenecks in industrial applications. This paper presents two methods to improve the medial surfaces computed from CT images of thin-plate mechanical objects. We first introduce a method for extending the ends of medial surfaces by finding the intersection points of medial voxels on the isosurface. We also propose a method to remove dent structures at junction edges by minimizing error functions. These improvements, integrated into a conventional medial surface extraction method using sub-sampling, resolve several drawbacks in reverse engineering applications.

KEYWORDS

Medial surface; Medial axis transforms; Reverse engineering; Shrinkage; Dent structure

1. Introduction

A medial axis [3] is the centerline skeleton of an input shape and is efficient for analyzing shapes, computer animation, and so on. In particular, the medial axes of 3D solid objects are represented by surface structures, which are also called *medial surfaces* (3D medial axis). In this paper, we focus on creating medial surfaces from volumetric images scanned by X-ray CT scanners.

Our motivation comes from reverse engineering applications. Reverse engineering uses geometric models of “real mechanical objects”. The geometric models are used for accelerating the manufacturing process, such as comparison with CAD models and CAE simulation of real objects [22]. The geometric models are usually created by isosurface extraction methods (e.g., [9]). This representation is efficient for solid objects. However, open surfaces are preferred for thin-plate objects, such as automobile bodies and plastic injections. In common CAD systems, open surfaces are represented as *mid-surfaces* [17, 18]. The medial surfaces of these thin-plate objects look similar to CAD models and some methods can create medial surfaces topologically equivalent to the input models. Thus, computing these medial surfaces is promising.

However, several issues still remain for computing medial surfaces from CT images for reverse engineering applications. First, the ends of medial surfaces are shrunk, or do not reach the ends of the input objects. This is because the medial axis by definition does not exist at the ends. As a result, errors of the dimensions need to be

corrected. The other issue is that small dents appear at junctions. This is also due to the definition of a medial axis. The diameters of inscribing spheres at junctions are relatively large and the difference makes a small dent at junctions. These artifacts, which cannot be seen in the surface models in common CAD systems, also need to be improved.

This paper presents two methods for improving medial surfaces in reverse engineering applications. These methods are based on a medial surface extraction method by sub-sampling [11]. The first method is a method for extending the shrunk medial voxels. The main idea is to add volumetric spheres to the input volume data so that their medial surfaces become extended medial surfaces of the input models. To add volumetric spheres, we introduce a method for estimating the intersection points between the extended medial axis and the isosurface of the object. The second method removes dent structures at junction edges. Our idea is to find new positions of junction vertices so that the positions are projected onto the planes defined by neighboring faces. This paper introduces a quadratic error-based function to find the positions.

The main advantage of the proposed methods is to improve the quality of medial surfaces computed from volumetric images for reverse engineering applications. Definition-based medial surfaces always create artifacts that become bottlenecks in reverse engineering. The result surfaces created by our methods do not follow the definition of medial axis. However, the resulting surfaces

look appropriate and they are efficient for reverse engineering applications.

2. Related work

Creating medial axes is known as medial axis transforms (MAT). MAT has a long history since Blum's work in 2D [3]. This section gives a review for constructing the medial axis from CT images.

One possible approach is the polygon-based approach; that is, medial surfaces are computed from the isosurface of CT images. For example, the use of Voronoi diagrams with surface points as sites can compute medial axes easily [1, 2, 4, 5]. However, the resulting surfaces are usually complicated or involve many branch structures. Simplified medial axis transforms have been introduced to efficiently remove these branches. For example, Foskey et al. [6] used separation angles to remove branches of medial axes and Sud et al. [21] improved the transforms so that homotopy of the object was preserved. The scale axis transform algorithm [8, 12] provides a simple and robust algorithm for simplification of medial axes by scaling the medial balls of the objects. However, these methods depend on the definition of medial axis and so are still sensitive to higher-valence branches or decomposition into a set of lower-valence junctions for isosurfaces. Similar problems are found for the chordal axis transform [14, 16], which also creates similar structures to the medial axis based on the connectivity of constrained Delaunay triangulations.

The alternative approach is to polygonize medial voxels, which are the voxel representation of medial axes. This approach usually binarizes input CT images and creates medial voxels by topological thinning. Topological thinning removes simple voxels that do not contribute to the topological changes, while the topology is preserved. However, the pruning strategy is a problem in this approach. For example, sequential thinning [19] iteratively removes simple voxels and parallel thinning [23] removes surface voxels. A main problem of these approach is to define the priority of pruning. Prohaska and Hege [15] obtained reasonable results by using the geodesic distance between two surface points that are the closest points of the voxels. Polygonization of medial voxels can be considered as surface reconstruction from a point set. However, many methods suppose the result to be two-manifold, whereas medial surfaces are non-manifold at junctions. Since medial voxels are aligned with a uniform voxel grid, it is possible to create triangles by connecting neighboring voxels, and the existence of ambiguous cases often creates small cavities at the junctions. Prohaska and Hege also introduced lookup tables for special cases, but the problems were not completely

resolved. Michikawa and Suzuki [11] introduced a sub-sampling method for polygonization of medial voxels. As a result of sub-sampling, the method simplifies the topological structure at junctions and can handle higher-valence junctions without unnecessary cavities. However, this method is also based on conventional medial axis transforms and so geometric artifacts still appear.

Mid-surfaces are often required for CAD models and some conversion methods from solid models have been studied. For example, Rezayat [18] introduced a method to find mid-surface patches for surface pairs across from each other and to create mid-surfaces by stitching these patches based on their adjacency graphs. The results are reasonable for our objective. However, it is difficult to apply this approach to scanned models, because it is difficult to find patch pairs and many patches have to be computed. In addition, this method requires human intervention for the selection of surface pairs. Ramanathan [17] introduced a method for computing mid-surfaces from a set of mid-curves defined on the faces. This method is also not suitable for scanned objects.

3. Brief overview of medial surface extraction by sub-sampling

Our method is based on the medial surface computation method by Michikawa and Suzuki [11]. In this section we give a brief overview of their method.

Their method is the polygonization of medial voxels by sub-sampling. This method, based on the method proposed by Prohaska and Hege [15], first computes medial voxels of the binary images from CT images of the object. Each medial voxel contains the distance value to the closest point on the isosurface. Next, we apply sub-sampling to find representative points of the medial voxels. When a point is selected, neighboring points within spherical support of the point with radius r are removed. Note that r is determined by the distance value at the point. We repeat this procedure until all medial voxels are sampled or removed. To preserve the topological structure, the points are sampled in the order of junction, boundary and surface voxels. These topological types are estimated by counting the number of connected components, as introduced by Malandain [10]. By following this order, junction points are preferentially selected. (A similar strategy for surface remeshing was introduced in [20].) Polygonal meshes are created by connecting sampled points based on Voronoi diagrams on medial voxels. (A similar strategy was introduced in [13] for meshing manifold surfaces from unorganized points.) The user's parameters are the isovalue t of the CT images and the thickness ϵ of the object.

4. Methods

An overview of our methods is shown in Fig. 1. Given a CT image (Fig. 1(a)), a binary image is computed by isovalue t (Fig. 1(b)). Next, medial voxels are computed from the binary image with thickness ϵ of the object (blue lines in Fig. 1(c)) by [15]. Since the medial voxels (blue lines in (c)) are shrunk so that they do not intersect the object's surface (black contour in (c)), we apply an extension method to the medial voxels (red lines in Fig. 1(d)) to their intersection points. A medial surface polygon is computed by the extended medial voxels (Fig. 1(e)) by [11]. Since the junction point is dented, we remove this to create smooth polygons (Fig. 1(f)). Our contributions presented in this paper are the extension of medial voxels (Fig. 1(d)) and dent removal (Fig. 1(f)). We describe these in the following subsections.

4.1. Extension of medial voxels

Simplified medial surfaces are usually shrunk and so we extend them so that the medial surface and the isosurfaces intersect (Fig. 2). Our idea is to estimate these

intersection points by using the initial medial voxels. Once the intersection points are found, we can add volumetric spheres of diameter ϵ at the intersection points. The result of the medial voxels is extended to the isosurface of the object.

The main issue of this step is to find the intersection points. To compute these points, we introduce a method based on region growing. Given the input binary image and its medial voxels (Fig. 2(a)), we classify the boundary voxels by their nearest medial voxels. We label the voxels if the nearest medial voxels are surface voxels (black lines in Fig. 2(b)). Estimation of the voxel topology is computed by counting the connected components [10]. The other boundary voxels are the nearest medial voxels (blue circles in Fig. 2(b)) and those not labeled yet (gray lines in Fig. 2(b)). Next, the labeled boundary voxels are segmented by the connected components and new labels are assigned to the voxels (red, yellow, and green lines in Fig. 2(c)). This segmentation shows to which sides the boundary voxels belong. Unlabeled voxels are labeled by region growing on the boundary voxels (bold colored lines in Fig. 2(d)). Here, the labeled voxels are used

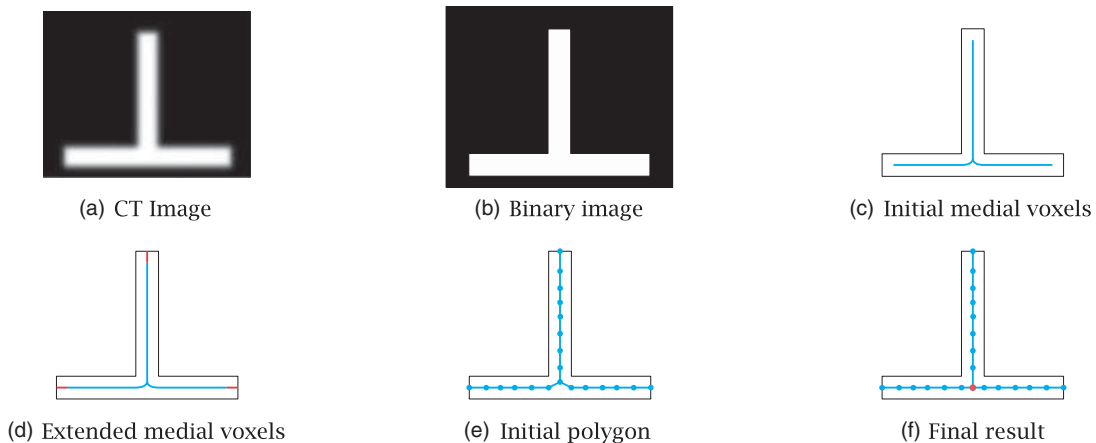


Figure 1. Overview of the proposed method illustrated in 2D.

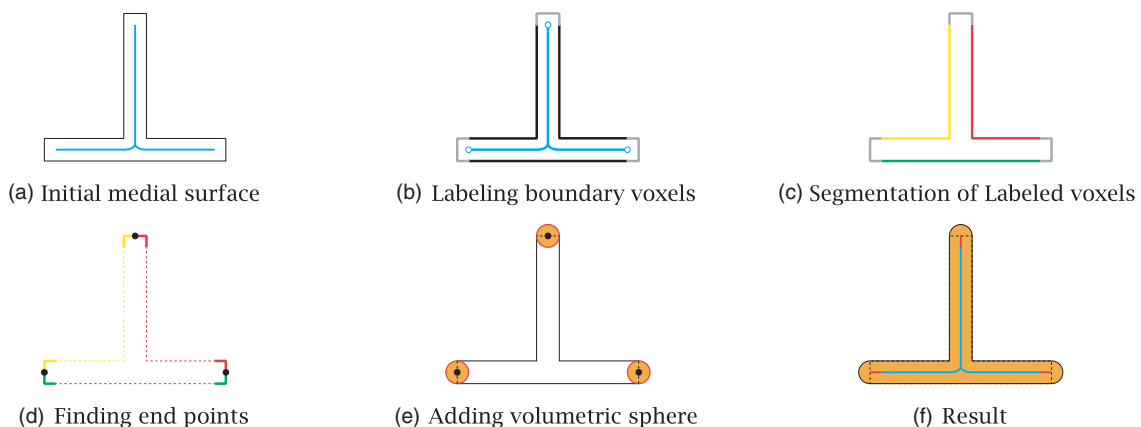


Figure 2. An overview of extension of medial surface (2D example).

as initial seeds. When the region growing is completed, we can find the intersection points where the difference labels meet (Fig. 2(d)), and these become the end points of the medial voxels. We now add volumetric spheres at these end points (orange circles in Fig. 2(e)). The diameter of each sphere is the same as the thickness parameter r . Finally, the medial voxel extraction method is applied again to the new binary image. The resulting medial voxels are extended to the isosurface of the original image (Fig. 2(f)).

4.2. Removing the dent structure at junction points

By definition of the medial axis, the diameters of inscribing spheres at the junctions are rather large. This causes the creation of dent structures at the junctions. We often use smoothing operators for meshes to smooth bumpy surfaces. However, such operators do not work well for non-manifold meshes.

The idea of removing a dent structure is to project junction points to neighboring surfaces. Let \mathbf{x}_i be a junction vertex. New vertex position $\hat{\mathbf{x}}_i$ can be computed

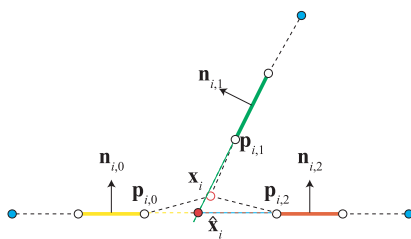


Figure 3. Removing dents at the junctions.

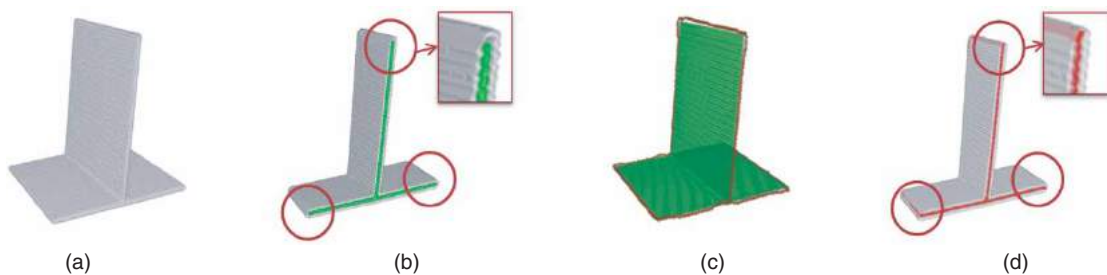


Figure 4. The result for T-shape.

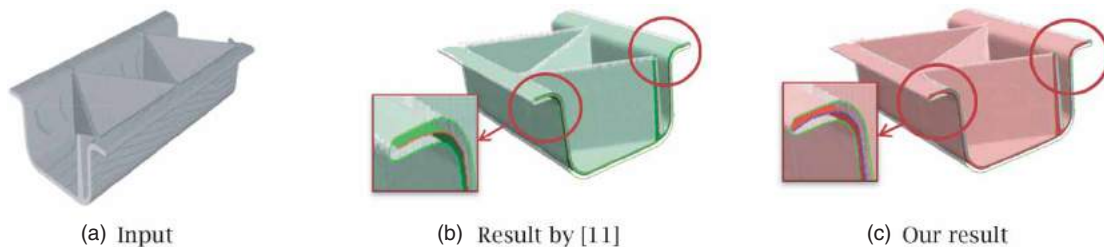


Figure 5. The result for member shape.

by minimizing Equation (1) based on the quadratic error metric [7]:

$$E(\hat{\mathbf{x}}_i) = \sum_j \langle \mathbf{n}_{i,j}, \hat{\mathbf{x}}_i - \mathbf{p}_{i,j} \rangle^2 + \|\mathbf{x}_i - \hat{\mathbf{x}}_i\|^2, \quad (1)$$

where $\langle \cdot, \cdot \rangle$ denotes the inner product, and $\mathbf{n}_{i,j}$ and $\mathbf{p}_{i,j}$ respectively denote the normal vector and a point of triangle f_j (Fig. 3). Note that no junction vertices belong to f_j . In Equation (1), the first term minimizes the difference between $\hat{\mathbf{x}}_i$ and a plane defined by f_j . Since the unique solution may not be computed in 3D by the first term, we add the second term so that the unique closest point is selected. Note that we can easily compute this for each vertex.

5. Results

5.1. Extension of medial voxels

The experimental results for the medial surface extensions are shown in Figs. 4 and 5. Both examples are metal sheet models scanned by industrial CT scanners. In Fig. 4, (a) shows the binary voxels, (b) shows a cutaway view of the shrunk medial voxels (green), (c) shows the end points (blue), and (d) shows the result (cutaway view). By comparing (b) with (d), we can confirm the medial voxels in (d) are slightly extended. Note that the medial voxels seem to be covered by gray voxel due to volume rendering, however the medial voxels are extended. Fig. 5 shows the result for a member (a car part). The cutaway result by the previous method [11] and the proposed method are shown in (b) (green)



Figure 6. Dent removal result.

and (c) (red), respectively. Transparent surfaces show an isosurface of the input data (a). We can confirm that the medial surface is extended to the isosurface in (c), whereas the result by a conventional method is shrunk.

5.2. Removing dent structure

The dent removal results for the T-shape and the member objects are shown in Fig. 6. For each subfigure, the left figure shows the original mesh and the right figure shows the smoothing results. We can confirm that the small dent structure (red arrow) in the right figure mostly disappear, whereas those in the right figure clearly exist. However, slight dents still remain in the results and they should be resolved in the future work.

5.3. Discussions

The computational time is summarized in Table 1. The experiment is conducted on a Windows PC with Intel Core i7 3.0 GHz. We can confirm that it takes about 20 minutes for computing the extended medial voxels, because we apply medial voxel extraction twice. In addition, our implementation is not yet fully optimized, and so performance improvement is expected. On the other hand, the computation time of dent removal is reasonable, because the computation for each vertex is independent.

Table 1. Statistics

Data (Fig.)	Volume Size	#faces	Extension [s]	Dent removal[s]
T-shape (4, 6(a))	240x240x140	7,461	1,190	7
member(5, 6(b))	210x210x298	31,596	1,240	36

The proposed methods involve some limitations. In extension method, we assume the CT images have enough margins for adding volumetric spheres. When the objects are connected by adding spheres, the topology of the medial surfaces will changed. In dent removal method, self-intersections may occur, since the method

does not take care of it. However, this can be seen at junction vertices and it can be resolved by smoothing methods in post processing. Finally, these methods do not have clear evaluation criteria yet, although the results are visually improved.

6. Summary and future work

We have presented two methods for removing the artifacts of medial surfaces computed from volumetric images of thin-plate models. We first introduced a method for extending medial voxels by adding volumetric spheres on the estimated intersection points of the extended medial voxels and the isosurface. To find the intersection points, we use region growing on boundary voxels. Initial seeds are extracted from the result of the shrunk medial surface. As a result, the medial surfaces reach the isosurface of the input models. We next introduced a method for smoothing the dent structure at the junctions. In this method, we proposed an error function defined by the distance between the junction point and the neighboring points. The dent structure can be removed by minimizing the error function. We also demonstrated that both proposed methods work well for several examples.

In addition to the limitations, we have some plans for future work. The proposed methods are currently integrated with a specific method [11]. However, we would like to integrate the methods with other medial surface extraction schemes. Other future work involves the extension of medial surfaces. Since volumetric spheres are added to binary images, some parts may be connected to each other. The divide-and-conquer approach may efficiently avoid such unexpected connections in binary images.

Acknowledgment

The authors would like to thank anonymous reviewers for valuable comments. This research was supported in part by JSPS KAKENHI (Grant No. 15K05761).

ORCID

Vaibhav Kumar  [http://orcid.org/\[0000-0003-2055-1945\]](http://orcid.org/[0000-0003-2055-1945])
 Takashi Michikawa  [http://orcid.org/\[0000-0002-0606-668X\]](http://orcid.org/[0000-0002-0606-668X])
 Hiromasa Suzuki  [http://orcid.org/\[0000-0003-4237-1101\]](http://orcid.org/[0000-0003-4237-1101])

References

- [1] Amenta, N.; Choi, S.; Kolluri, R. K.: The power crust, Proceedings of ACM symposium on solid modeling and applications, 2001, 249–66. <http://dx.doi.org/10.1145/376957.376986>
- [2] Attali, D.; Montanvert, A.: Computing and simplifying 2D and 3D continuous skeletons, *Computer Vision and Image Understanding*, 67(3), 1997, 261–273. <http://dx.doi.org/10.1006/cviu.1997.0536>
- [3] Blum, H.: *A transformation for extracting new descriptors of shape*, *Models for the perception of speech and visual form*, The MIT Press, Cambridge, 1967, 326–380.
- [4] Dey, T.K.; Zhao, W.: Approximate medial axis as a Voronoi subcomplex, *Proceedings of ACM symposium on solid modeling and applications*, 2002, 356–66. <http://dx.doi.org/10.1145/566282.566333>
- [5] Etzion, M.; Rappoport, A.: Computing the Voronoi diagram of a 3-D polyhedron by separate computation of its symbolic and geometric parts, Proceedings of the fifth ACM symposium on solid modeling and applications, 1999, 167–78. <http://dx.doi.org/10.1145/376957.376986>
- [6] Foskey, M.; Lin, M. C.; Manocha, D.: Efficient computation of a simplified medial axis, Proceedings of ACM symposium on solid modeling and applications, 2003, 96–107. <http://dx.doi.org/10.1145/781606.781623>
- [7] Garland, M.; Heckbert, P.S.: Surface simplification using quadric error metrics, *Proceedings of SIGGRAPH97*, 1997, 209–216. <http://dx.doi.org/10.1145/258734.258849>
- [8] Giesen, J.; Miklos, B.; Pauly, M.; Wormser, C.: The scale axis transform. *Proceedings of symposium on computational geometry*, 2009, 106–15. <http://dx.doi.org/10.1145/1542362.1542388>
- [9] Lorensen, W. E.; Cline, H. E.: Marching Cubes: A high resolution 3D surface construction algorithm, *Computer Graphics*, 21(4), 1987, 163–169. <http://dx.doi.org/10.1145/37401.37422>
- [10] Malandain, G.; Bertrand, G.; Ayache, N.: Topological segmentation of discrete surfaces, *International Journal of Computer Vision*, 10(2), 1993, 183–197. <http://dx.doi.org/10.1007/BF01420736>
- [11] Michikawa T.; Suzuki H.: Polygonization of volumetric skeletons with junctions, *Computer-Aided Design*, 45(4), 2013, 822–828. <http://dx.doi.org/10.1016/j.cad.2011.06.003>
- [12] Miklos, B.; Giesen, J.; Pauly, M.: Discrete scale axis representations for 3D geometry, *ACM Transactions on Graphics*, 29, 2010, 101:1–101:10. <http://dx.doi.org/10.1145/1778765.1778838>
- [13] Ohtake Y.; Belyaev A.; Seidel H-P.: An integrating approach to meshing scattered point data, *Proceedings of the 2005 ACM symposium on solid and physical modeling*, 2005, 61–69. <http://dx.doi.org/10.1145/1060244.1060252>
- [14] Prasad, R.: Morphological Analysis of Shapes, *CNLS Newsletter*, 139, 1997, 1–18.
- [15] Prohaska S.; Hege, H.C.: Fast visualization of plane-like structures in voxel data, *Proceedings of Visualization '02*, 2002, 29–36. <http://dx.doi.org/10.1109/VISUAL.2002.1183753>
- [16] Quadros W. R.: An approach for extracting non-manifold mid-surfaces of thin-wall solids using chordal axis transform, *Engineering with Computers*, 24(3), 2008, 305–319. <http://dx.doi.org/10.1007/s00366-008-0094-1>
- [17] Ramanathan M.; Gurumoorthy B.: Generating the Mid-surface of a solids using 2D MAT of its faces, *Computer-Aided Design and Applications*, 1(1–4), 2004, 665–674. <http://dx.doi.org/10.1080/16864360.2004.10738312>
- [18] Rezayat M.: Mid-surface abstraction from 3D solid models: general theory and applications, *Computer-Aided Design*, 28(11), 1996, 905–915. [http://dx.doi.org/10.1016/0010-4485\(96\)00018-8](http://dx.doi.org/10.1016/0010-4485(96)00018-8)
- [19] Saito, T.; Toriwaki, J.: A sequential thinning algorithm for three dimensional digital pictures using the Euclidean distance transformation, *Proceedings of the 9th Scandinavian conference on Image Analysis*, 1995, 507–516.
- [20] Shimada, K.; Gossard, D. C.: Bubble mesh: automated triangular meshing of non-manifold geometry by sphere packing, *Proceedings of ACM symposium on solid modeling and applications*, 1995, 409–19. <http://dx.doi.org/10.1145/218013.218095>
- [21] Sud, A.; Foskey, M.; Manocha, D.: Homotopy-preserving medial axis simplification, *Proceedings of ACM symposium on solid and physical modeling*, 2005, 39–50. <http://dx.doi.org/10.1145/1060244.1060250>
- [22] Suzuki, H.; Fujimori, T.; Michikawa, T.; Miwata, Y.; Sadaoka, N.: Skeleton surface generation from volumetric models of thin plate structures for industrial applications, IMA conference on the mathematics of surfaces, LNCS, 4647. 2007. 442–464. http://dx.doi.org/10.1007/978-3-540-73843-5_27
- [23] Tsao, Y. F.; Fu, K.S.: A parallel thinning algorithm for 3-D pictures, *Computer Graphics and Image Processing*, 17(4), 1981, 315–31. [http://dx.doi.org/10.1016/0146-664X\(81\)90011-3](http://dx.doi.org/10.1016/0146-664X(81)90011-3)